New Monodense Large Pore Silica-Based Materials for the Analysis of Biomacromolecular Compounds by Reversed-Phase Liquid Chromatography

V. K. Langsi, J. L. McGrath, J. J. Hogan, S. Analakkattillam, J. P. Hanrahan
Glantreo Ltd, ERI Building, Lee Road, Cork City, T23XE10, Ireland. www.glantreo.com info@glantreo.com

Introduction

Over the last decade there have been significant advances in the development of mon-odisperse large pore (400-1000Å) silica particles, designed either as fully porous (FPP) or superficially porous particles (SPP), to facilitate the reversed-phase separation of bi-omacromolecules such as intact large proteins. Columns packed with such particles have demonstrated superior resolutions accompanied by lower column back pressures during these separations compared to smaller pore materials of the same particle size [1, 2, 3].

The selection of the optimal particle size, stationary phase chemistry and particle design impacting chromatographic efficiency can minimise the mass transfer effect when using large pore particles [4]. Macromolecules can move rapidly in and out of the shell layer of porous shell particles with large pore sizes, resulting in reduced band broadening at higher mobile phase velocities. SPP particles exhibit advantages with biomacromolecules for fast separations at high mobile phase velocities because of superior mass transfer (kinetic) properties (i.e. smaller van Deemter C term) [5]. The thickness of the porous layer determines the size range of analyte molecules that would enter the pore structure with minimum restriction for interaction with the appropriate stationary phase. The larger the pore size the more macromolecular molecules would access the internal pore volume with unrestricted diffusion, thereby increasing efficiency and column performance. For example a SPP particle with 160 Å pores, specifically designed for separating peptides and small proteins. This column is capable of delivering good efficient peak shapes for ribonuclease A (13.7 kDa) but yields poor peak shapes with poor efficiency for solute molecules above 15 kDa molecular weight. Whereas, particles with pore sizes >400Å have been demonstrated to separate large proteins greater than 400 kDa [1, 6].

Monodensity in silica structure has also been demonstrated to have an effect on the mass transfer of large molecules which could otherwise lead to peak broadening, peak tailing and subsequent loss in chromatographic efficiency. The production of monodense particles has been reported in a previous publication [7] Silica particles possessing a monodense structure with a homogeneous internal pore structure would allow for more efficient and rapid diffusion of large solute molecules into and out of the silica pore structure resulting in a more efficient and effective chromatography. It has also been shown that it is easier to pack monodense silica particles compared to traditional silicas as a result of the homogeneous distribution of particles during the packing process [7]. Moreover, large pore spherical monodense particles with low pore volumes have been researched to experience reduced inter and intraparticle tortuosity which increases diffusion and permeability of solutes [8].

In addition to having a large pore size and monodense structure, the retention capacity, selectivity and efficiency of these new particles is also influenced by the type of alkyl bonded stationary phase. Joseph K. Kirkland et al have demonstrated that different macromolecules such as peptides and proteins would have different retention and selectivity on wide-pore SPP columns containing C4, C8 and C18 stationary phases using acetonitrile/aqueous trifluoroacetic acid (TFA) mobile phase. Using a six-protein mixture comprised of ribonuclease A-(13.7kDa), cytochrome C (12.4kDa), Bovine Serum Albumin-(66.4kDa), apomyoglobin-(17kDa), enolase-(46.7kDa) and phosphorylase B-(97.2kDa), they demonstrated only a minor difference in peak shape and yield on C8 and C4 phases. However, the shorter C4 phase showed slightly greater retention due to its higher ligand density on the silica base support (4.2 µmol/m^2 for 0.88% carbon) compared to a bulkier C8 phase (2.0 µmol/m^2 for 0.92% carbon) [1].

Between 2009 and 2014 Advanced Material Technology (AMT) continued to lead the development and commercialisation of HALO® BioClass material with the release of 2.0µm particle size, 400Å pore size, material for the analysis of large molecules. The first 1000Å superficially porous 2.7µm particle with a shell thickness of 0.5µm and

$22m^2g^{-1}$ surface area was developed by Boyes and Kirkland in 2017 intended for reversed-phase separations of very large proteins and monoclonal antibodies (mAbs) [10,11].

Most methods for the separation of proteins by RP-HPLC use acidic mobile phase additives, e.g. formic and trifluoroacetic acid, in both the aqueous (A solvent) and organic (B solvent) components of the mobile phase system. The organic modifier frequently consists of acetonitrile, or acetonitrile with a short aliphatic alcohol (propanol, butanol or isopropanol) which is added to increase the elutropic strength of the B solvent. In addition to using an organic gradient, elevated column temperature (40-90°C) is frequently employed to deliver the desired chromatographic profile [1].

In this report two newly synthesised monodense particles are described with a wide pore structure (400-1000Å); the SOLAS™ 1.7µm (Glantreo, Cork, Ireland) fully porous particle (FPP) and EIROSHELL™ a 2.6µm (Glantreo, Cork, Ireland) superficially porous particle (SPP). Both materials are designed specifically to separate proteins and other biomacromolecules up to approximately 150 kDa. These new materials were bonded with a short butyl silane (C4) stationary phase and demonstrated high efficiency for the separation of large protein molecules which rapidly enter the porous structure, are adsorbed on the stationary phase and then desorb resulting in reduced band broadening.

Experimental

The SOLAS™ and EIROSHELL™ particles are manufactured via a modified Stöber process [7]. The particulars of this process and subsequent bonding and packing protocols are a trade secret to the company.

- The external morphology of the particles was examined by using scanning electron microscopy (SEM) [FEI Inspect F, (Hillsboro, Oregon USA)] operating at 10 kV. The surface area, pore size, pore size distribution and pore volume measurements of the particles were performed based on the nitrogen gas sorption method using a Micromeritics Tristar II (Micromeritics, Norcross, CA, USA) sur-face and pore size analyser.
- The particle size distribution was determined by an electric sensing zone technique based on the Coulter principle on a Multitier 4e Coulter counter (Fullerton, CA, USA) instrument. A CE 440 fully automated elemental analyser (Exeter Analytical Inc., North Chelmsford, MA, USA) with thermal conductivity detection was used to determine the elemental analysis of the C4 bonded FPP and SPP particles.

Using an in house packing technique, stable reversed phase C4 columns were packed that can be applicable for separating large molecular weight compounds such as proteins and peptides. HPLC performance and biomacromolecule application evaluations were carried out using an Agilent 1200 LC (Santa Clara, CA) and Jasco LC 4000 (Easton, MD) series systems. Flow rates of 0.2ml/min were used for all columns which had dimensions of 2.1mm ID x 50mm. (John Shepard, Shepherd Hardware, PA, USA)

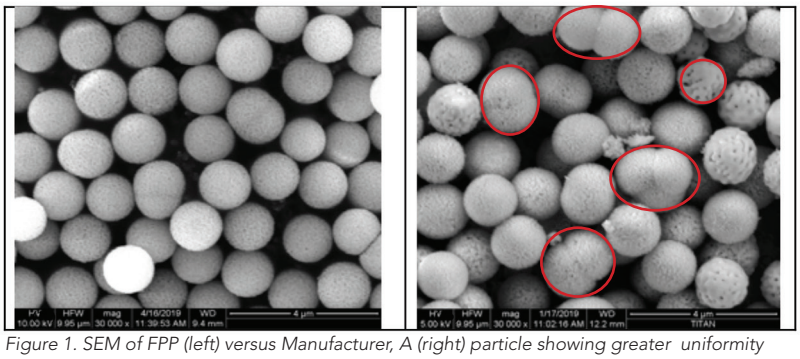

Figure 1. SEM of FPP (left) versus Manufacturer, A (right) particle showing greater uniformity of porosity in the SOLAS spheres. Notice the fine spherical structure in (1a) compared to agglomerated, uneven particle sizes in (1b) circled in red.

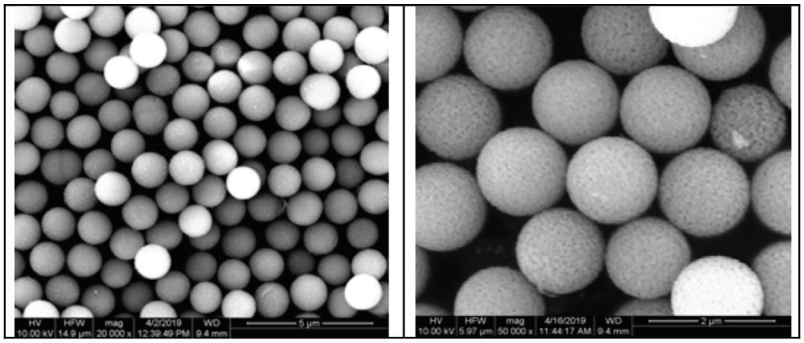

Figure 2. SEM images of FPP 1.7µm monodense particles.

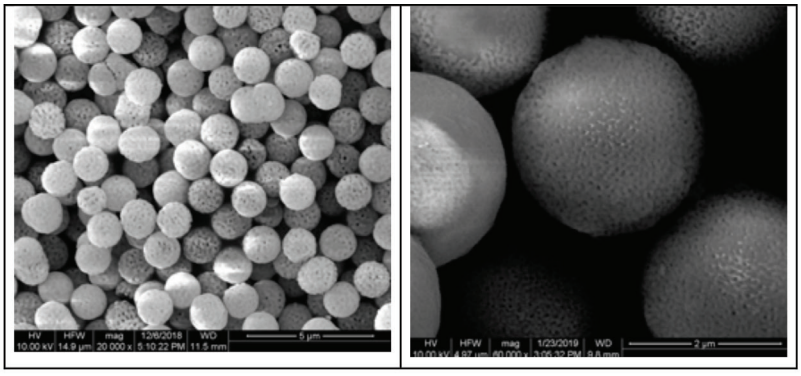

Figure 3. SEM and FIB images of SPP particle.

Results

Fully porous and superficially porous particles synthesised for the purpose of this report are based on existing technologies to yield spherical and monodense particles with wide pores for optimum biomacromolecule chromatographic efficiency.

Scanning electron microscopy (SEM) results after the particles have been manufactured are shown in Figure (1a) for FPP 1.7µm particle and (1b) for Manufacturer A 1.7µm particle.

The FPP particle in Figure 1a is more monodense than the other Manufacturer particle in Figure1b and this has been shown in previous work to give better column efficiency [6].

Figure 2 shows the SEM images for 1.7µm FPP while Figure 3 illustrates the SEM images of 2.6µm SPP. The new SPP prepared in this report is comprised of the solid core (1.9µm) and porous shell (350nm) structure. The SEM images show the wide-pore and ultra-wide pore structures to be just about visible and evenly distributed within the particles. The particle size distribution of

Table 1. The physiochemical properties of wide pore and ultra-wide pore FPP and SPP particles

Particle type	Particle size (µm)	Surface area (m^2g^{-1})	Average pore volume (cm^3g^{-1})	Average pore size (Å)	%C	Surface coverage (α) (µmol/nm^2)	Monodispersivity (d90/d10)
Competitor 400A	1.7	65	0.6	300	n/d	n/d	1.7
FPP 400Å	1.7	41	0.2	430	0.69	2.2	1.3
FPP 1000Å	1.7	22	0.1	950	0.33	2.1	1.3
SPP 500Å	2.6	15	0.05	430	0.32	2.9	1.2
SPP 1000Å	2.6	9	0.05	1200	0.15	2.3	1.2

the FPP and SPP is shown on the size distribution graph Figure 4. The data obtained from this technique can also be used to calculate the mean, median and particle distribution ratio (d90/d10).

Table 1 summarises the physiochemical properties of a range of 1.7µm FPP and 2.6µm SPP synthesised with wide (400-500Å) and ultra-wide pores (1000Å) respectively. The table also lists the physical properties of a competitor brand of large pore silicas. For the efficient separation of macromolecules, it is suggested that the particle pore size for optimal chromatographic separation should be in the order of at least 10 times the effective hydrodynamic diameter of an analyte. All particles have monodispersity (d90/d10) values ≤ 1.3 indicating they are monodispersed and do not aggregate as evidence from SEM and FIB micrographs, Figures 1a, 2 and 3.

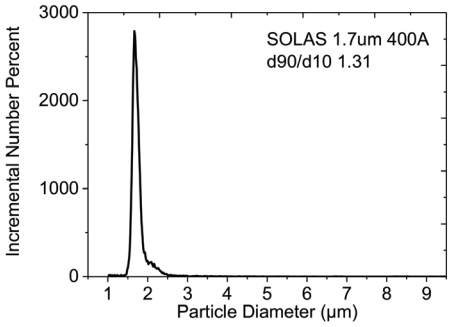

Figure 4. Particle size distribution curve for an ultra-wide pore 1.7µm particle.

Figure 5 illustrates the pore size distribution profiles for FPP 1.7µm and SPP 2.6µm with the numerical values for FPP 1.7µm and SPP 2.6µm shown in Table 1. The two SPP 2.6µm particles (500Å and 1000Å) have the same low average pore volume of 0.05cm^3g^{-1}, while the average pore volume of the FPP 1.7µm 400Å particle (0.20 cm^3g^{-1}) is double that for FPP 1.7µm 1000Å particle (0.10 cm^3g^{-1}).

For the wide-pore particles (i.e. FPP 1.7µm 400Å and SPP 2.6µm 500Å) the pore volume increases to maximum pore expansion and then begin to decrease as pore size continue to increase. For ultra-wide pore particles (i.e. FPP 1.7µm 1000Å and SPP 2.6µm 1000Å), there is steady increase in pore volume with increase in pore size to maximum pore expansion. The average pore size distribution was calculated using the Kelvin equation derived from the Barrett-Joyner-Halenda (BJH) model [13].

Application evaluation for SOLAS™ FPP and EIROSHELL™ SPP columns

Gradient separation of a mixture of six standard protein compounds (in eluting order: 1. ribonuclease A (14.70kDa) 80µg/ml, 2. cytochrome C (12.33kDa) 110µg/ml, 3. BSA (66.43kDa) 400µg/ml, 4. myoglobin (16.71kDa) 250µg/ml, 5. enolase (67.00kDa) 430µg/ml, and 6. phosphorylase B (97.20kDa) 1.18µg/ml are compared in Figure 6 for wide-pore FPP 1.7µm C4-400Å and SPP 2.6µm C4-500Å columns, plus ultra-wide pore FPP 1.7µm C4-1000Å, and SPP 2.6µm C4-1000Å columns as shown in Figure 6.

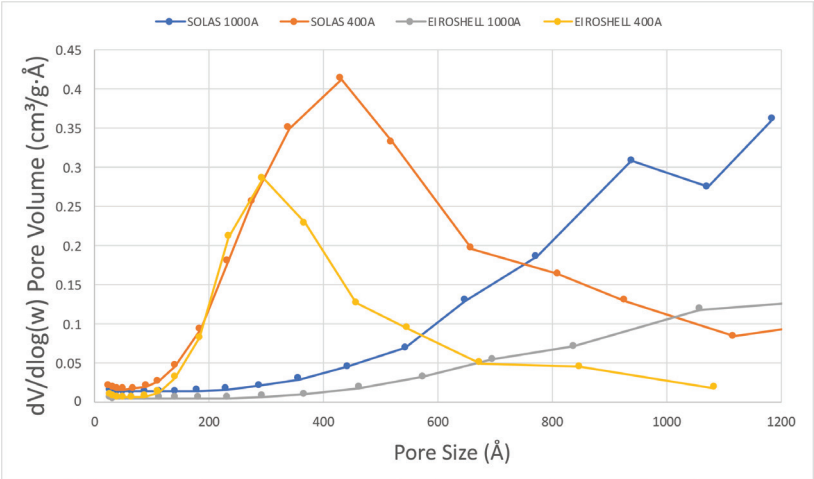

Figure 5. BJH pore size distribution curves. It should be noted that the pore volume decreases as pore size increases after pore expansion.

All peaks for the wide-pore FPP 1.7µm C4-400Å column (Fig. 6A) show a slightly longer retention time (Table 3a) compared to the ultra-wide FPP 1.7µm C4-1000Å column (Figure 6B & Table 3b), suggesting some restricted diffusion of these large protein molecules in the relatively smaller pore particles. The protein macromolecules ribonuclease A and cytochrome C have better separation efficiencies (based on the number of theoretical plates, NTP) on FPP 1.7µm C4-400Å than on FPP 1.7µmC4-1000Å columns (Tables 3a and 3b). This can be attributed to the larger particle surface area 41 m^2g^{-1}, and subsequently higher %C 0.69 of FPP 1.7µm C4-400Å compared to 22 m^2g^{-1} and %C 0.33 for FPP 1.7µm C4-1000Å (Table 1). FPP 1.7µm C4-1000Å shows a better efficiency for phosphorylase B compared to FPP 1.7µm C4-400Å as seen by the number of theoretical plates in Tables 3a & 3b. This is due to the restricted diffusion of the large molecular weight phosphorylase B (97.20kDa) through the relatively smaller pore size FPP 1.7µm C4-400Å compared to the ultra-wide FPP 1.7µm C4-1000Å particle.

For SPP columns, compared to SPP 2.6µm C4-500Å (Figure 8C), SPP 2.6µm C4-1000Å (Figure 6D) show higher retention times and efficiency in terms of number of theoretical plates (Tables 3c & 3d) for ribonuclease A, cytochrome C, BSA and myoglobin. This is due to the larger pore size for SPP 2.6µm C4-1000Å which causes the unrestricted diffusion of these protein macromolecules. The separation efficiency (NTP) of the protein macromolecule, enolase in both columns (Tables 3c and 3d) are close, suggesting that the diffusion restriction due to pore size does not have an adverse band broadening effect for this analyte. SPP 2.6µm C4-500Å shows a better efficiency for phosphorylase b compared to SPP 2.6µm C4-1000Å indicating an added benefit of SPP 2.6µm C4-500Å with a larger surface area (15m^2g^{-1}) compared to SPP 2.6µm C4-1000Å (9m^2g^{-1}) as seen in Table 1.

Effect of Large Pore Monodense Particles on Separation of Biomolecules

Figure 7 below illustrates the resolving

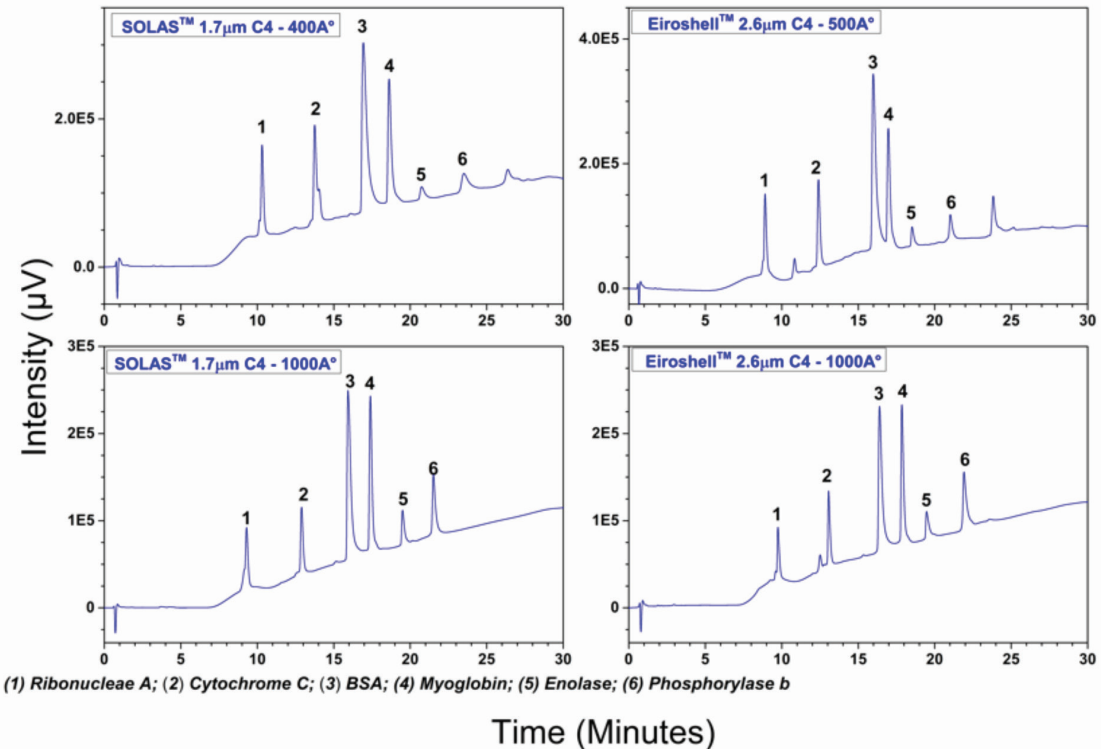

Figure 6. Comparison of chromatographic separation of protein mixture on four columns. (A) wide-pore fully porous FPP 1.7µm C4-400Å, (B) ultra-wide pore fully porous FPP 1.7µm C4-1000Å, (C) wide-pore superficially porous SPP 2.6µm C4-500Å, and (D) ultra-wide pore superficially porous SPP 2.6µm C4-1000Å columns. All columns have the same dimension 2.1mm ID x 50mm, and chromatographic condition: mobile phase A: 0.1% TFA in water & B: 0.075%TFA in 100% acetonitrile, gradient 20-70% B in 25min, temperature 60°C, flow rate 0.2ml/min, injection volume 5.0uL, UV 220nm

Table 3a. Peak information for FPP 1.7µm 400Å.

Peak #	tR(min)	NTP	Resolution	Symmetry factor
1	10.312	25633	N/A	1.508
2	13.753	39455	12.906	1.281
3	16.934	14817	7.654	2.807
4	18.616	37091	3.577	2.295
5	20.745	28798	4.875	1.590
6	23.506	16896	4.567	1.451

Table 3b. Peak information for FPP 1.7µm 1000Å.

Peak #	tR(min)	NTP	Resolution	Symmetry factor
1	9.301	15599	N/A	0.835
2	12.898	31716	12.277	1.469
3	15.932	24431	8.724	2.811
4	17.394	51705	4.107	1.862
5	19.499	68888	7.001	2.007
6	21.516	65693	6.391	1.733

Table 3c Peak information for SPP 2.6µm C4-500Å.

Peak #	tR(min)	NTP	Resolution	Symmetry factor
1	8.909	17846	N/A	1.368
2	12.401	27001	12.313	1.558
3	15.982	21959	9.792	2.429
4	16.967	41156	2.579	2.053
5	18.516	60190	4.881	2.000
6	21.020	59494	7.765	1.226

Table 3d. Peak information for SPP 2.6µm C4-1000Å.

Peak #	tR(min)	NTP	Resolution	Symmetry factor
1	9.751	29974	N/A	1.838
2	13.065	46978	14.245	1.821
3	16.392	28796	10.634	2.420
4	17.854	60225	4.328	2.138
5	19.468	55566	5.210	2.113
6	21.912	52631	6.880	2.181

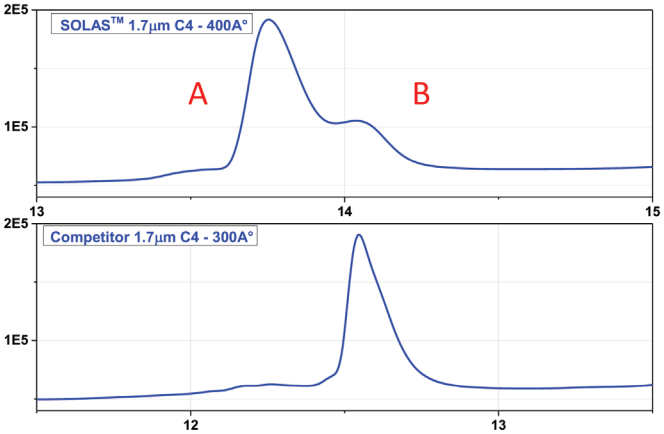

Figure 7. Comparison of chromatographic separation of Cytochrome C on wide-pore fully porous FPP 1.7µm C4-400Å compared to the competitor 1.7µm C4-300Å column. Both columns have the same dimension 2.1mm ID x 50mm, and chromatographic condition: mobile phase A: 0.1% TFA in water & B: 0.075%TFA in 100% acetonitrile, gradient 20-70% B in 25min, temperature 60°C, flow rate 0.2ml/min, injection volume 5.0uL, UV 220nm.

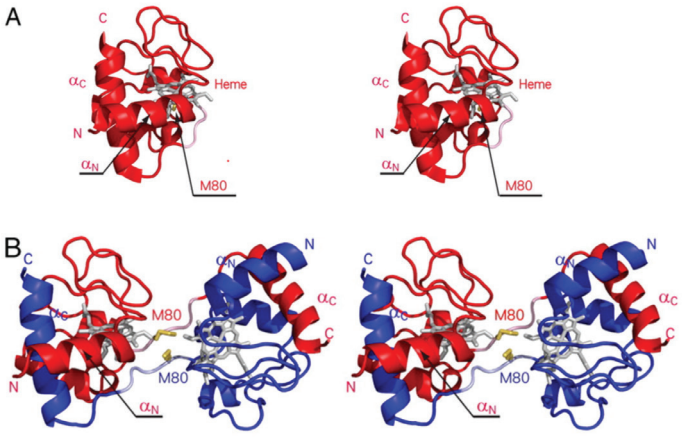

Figure 8. Schematic representations of crystal structures of oxidised monomeric and oligomeric cyt c. (A) Structure of monomeric cyt c (PDB ID code 1HRC). (B) Structure of dimeric cyt c (red and blue).

power of the new large pore monodense FPP 1.7um 400A material compared to that of a traditional 300Å material. Figure 9 shows a separation of Cytochrome C it is evident that a side peak is clearly present (as denoted by 'B' at 14.1 mins, which is not present for the competitor columns. These side peaks are possibly a higher order of aggregate impurities (or polymeric versions of Cytochrome C) present in the Cytochrome C. Interconversion of monomers and polymers in Cytochrome c has been known for nearly half a century, but the mechanism of its polymerisation is still unknown due to a lack of information on the structural and thermodynamic characteristics of the oligomerization process. The large pore FPP 1.7um 400A has a higher sensitivity to these impurities compared to the competitive column. Similar results are noted for monoclonal antibodies (mAbs) however the data is currently in publication elsewhere. The structures for A (monomeric) and B polymerics Cytochrome C are shown in Figure 8.

Conclusion:

New wide-pore and ultra-wide pore fully porous and superficially porous silica particles have been synthesised and surface treated with dimethyl butyl stationary phase for the separation of large protein molecules. The new materials proved to be stable with improved efficiency and peak shapes when employing low pH mobile phases containing additives like Trifluoroacetic acid (TFA) and Formic acid (FA) at high temperatures (40-60°C). The high column efficiency of the fully porous particle (FPP 1.7µm C4-400Å) compared to its commercially available competitive counterpart is primarily due to the narrow particle size distribution ratio and the large surface area which contributed to effective sample loading. The ultra-wide pore superficially porous particle (SPP 2.6µm C4-1000Å) showed more sensitivity to aggregate impurities in cytochrome C compared to its competitive counterpart. These materials should find wide application in biopharmaceutical separations determining the purity of new drugs where high speed, high sensitivity and efficient separations without a drastic increase in column pressure are important.

References

1. B. M. Wagner, S. A. Schuster, B. E. Boyes, J. J. Kirkland, Superficially porous silica particles with wide pores for biomacromolecular separations, J. Chromtogr. A, 1264 (2012) 22-30
2. S. A. Schuster, B. M. Wagner, B. E. Boyes, J. J. Kirkland, Wider pore superficially porous particles for peptide separations by HPLC, J. Chromatogr. Sc. Vol. 48, Advanced Material Technology, Inc. Wilmington, DE 19810, August 2010.
3. LCGC North America, vol. 35, issue 4, April 2017, pages 22-23
4. A. Astefanei, I. Dapic, M. Camenzuli, Different Stationary Phase Selectivities and Morphologies for Intact Protein Separations, Chromatographia 2017, 80(5), 665-687
5. V.K.Langsi, B. A. Ashu-Arrah, J. D. Glennon, Sub-2-µm seeded growth mesoporous thin shell particles for high-performance liquid chromatography: Synthesis, functionalisation and characterisation, J. Chromatogr. A, 1402 (2015) 17-26.
6. S. A. Schuster, Improve your monoclonal antibody separations by leveraging the advantages of Fused-core column, Advance Material Technology, Inc. Wilmington, DE 19810, July 15, 2018
7. J. P. Hanrahan, T. O'Mahony, R. Curley, J. J. Hogan, J. M. Tobin, An introduction to the concept of monodensity in silica particles and its effect on chromatographic performance, Chromatography Today, February/March 2017
8. M. Barrande, R. Bouchet, and R. Denoyel, Tortuosity of Porous Particles, Anal. Chem. 2007 (79), 9115-9121
9. R. Takahashi, S. Sato, T. Sodesawa and H. Nishida, Effect of pore size on the liquid-phase pore diffusion of nickel nitrate, PCCP 2002, issue 15.
10. European patent office number EP2365997B1 https://patents.google.com/patent/EP2365997B1/en)
11. E. Olah, S. Fekete, J. Fekete, K. Ganzler, Comparative study of new shell-type sub-2µm fully porous and monolith stationary phases focusing on mass transfer resistance, J. Chromatogr. A, 1217 (2010) 3642-3653
12. F. Gritti, I. Leonardis, D. Shock, P. Stevenson, A. Shalliker, G. Guiochon, Performance of columns packed with the new shell particles, Kinetex-C18J. Chromatogr. A, 1217 (2010) 1589-1603.
13. E.P. Barrett, L.G. Joyner, P.P. Halenda, The Determination of Pore Volume and Area Distributions in Porous Substances. I. Computations from Nitrogen Isotherms, J. Am. Chem. Soc., 73 (1951) 373-380.
14. N. Marchetti, A. Cavazzini, F. Gritti, G. Guiochon, J. Chromatogr. A. 1163 (2007), 203-211